

1

2 ***In vitro* profiling of orphan G protein coupled receptor (GPCR)**  
3 **constitutive activity**

4

5 **Lyndsay R. Watkins and Cesare Orlandi \***

6 Department of Pharmacology and Physiology, University of Rochester Medical Center,  
7 Rochester, NY 14642, USA

8 \* Correspondence: [cesare\\_orlandi@urmc.rochester.edu](mailto:cesare_orlandi@urmc.rochester.edu)

9

10

11

12

13

14

15

16

17

18

19

20 **Running title:**

21 Orphan GPCR constitutive activity

22

23 **Keywords:**

24 G protein-coupled receptor (GPCR); constitutive activity; cell signaling; molecular pharmacology.

25 **Abstract**

26 **Background and Purpose**

27 Members of the G protein coupled receptor (GPCR) family are targeted by a significant fraction  
28 of the available FDA-approved drugs. However, the physiological role and pharmacological  
29 properties of many GPCRs remain unknown, representing untapped potential in drug design. Of  
30 particular interest are ~100 less-studied GPCRs known as orphans because their endogenous  
31 ligands are unknown. Intriguingly, disease-causing mutations identified in patients, together with  
32 animal studies, have demonstrated that many orphan receptors play crucial physiological roles,  
33 and thus, represent attractive drug targets.

34 **Experimental Approach**

35 The majority of deorphanized GPCRs demonstrate coupling to  $G_{i/o}$ , however a limited number of  
36 techniques allow the detection of intrinsically small constitutive activity associated with  $G_{i/o}$  protein  
37 activation which represents a significant barrier in our ability to study orphan GPCR signaling.  
38 Using luciferase reporter assays, we effectively detected constitutive  $G_s$ ,  $G_q$ , and  $G_{12/13}$  protein  
39 signaling by unliganded receptors, and introducing various G protein chimeras, we provide a  
40 novel, highly-sensitive tool capable of identifying  $G_{i/o}$  coupling in unliganded orphan GPCRs.

41 **Key Results**

42 Using this approach, we measured the constitutive activity of the entire class C GPCR family that  
43 includes 8 orphan receptors, and a subset of 20 prototypical class A GPCR members, including  
44 11 orphans. Excitingly, this approach illuminated the G protein coupling profile of 8 orphan GPCRs  
45 (GPR22, GPR137b, GPR88, GPR156, GPR158, GPR179, GPRC5D, and GPRC6A) previously  
46 linked to pathophysiological processes.

47 **Conclusion and Implications**

48 We provide a new platform that could be utilized in ongoing studies in orphan receptor signaling  
49 and deorphanization efforts.

50 **What is already known**

- 51
  - A large group of understudied orphan GPCRs controls a variety of physiological process.

52 **What this study adds**

- 53
  - A new strategy to identify G protein signaling associated with orphan GPCRs.

54 
  - Identification of  $G_{i/o}$  coupling for 8 orphan GPCRs.

55 **What is the clinical significance**

- 56
  - Many orphan GPCRs are associated with pathological conditions and represent promising

57 
  - druggable targets.

58

59 **1. INTRODUCTION**

60 The large family of G protein coupled receptors (GPCRs) constitutes the most exploited  
61 drug target in the human genome (Hauser, Attwood, Rask-Andersen, Schioth, & Gloriam, 2017;  
62 Sriram & Insel, 2018). This is the result of GPCR involvement in the regulation of key physiological  
63 processes combined with accessibility at the plasma membrane. Nonetheless, the endogenous  
64 ligands of many GPCRs have yet to be identified, which collectively are referred to as orphan  
65 GPCRs (oGPCRs). In spite of the lack of known endogenous ligands, experimental evidence from  
66 both animal models and human studies suggest that many oGPCRs regulate important  
67 physiological processes and therefore represent attractive therapeutic targets that remain to be  
68 exploited (Audo et al., 2012; Peachey et al., 2012; Wang et al., 2019; Watkins & Orlandi, 2020).  
69 The first critical step towards the deorphanization of an oGPCR involves identifying the  
70 intracellular signaling pathways that it modulates, thereby providing an essential readout to build  
71 screening platforms aimed at testing receptor activation by candidate endogenous/synthetic  
72 ligands. However, the lack of known ligands significantly limits the experimental strategies that  
73 can be applied to identify oGPCR-activated signaling pathways, thereby representing one of the  
74 greatest difficulties in studying oGPCRs. Although not widely utilized, one way to address this  
75 question involves measuring the GPCR constitutive activity (Bond & Ijzerman, 2006; Ngo,  
76 Coleman, & Smith, 2015). Constitutive activity is observed when a GPCR produces spontaneous  
77 G protein activation in the absence of agonist (Rosenbaum, Rasmussen, & Kobilka, 2009), a  
78 property often observed when overexpressing GPCRs in heterologous systems and also detected  
79 *in vivo* (Corder et al., 2013; Damian et al., 2012; Inoue et al., 2012). Given that current available  
80 assays have been unsuccessful in illuminating G protein coupling profiles for many oGPCRs, in

81 particular in detecting those dominantly coupling to  $G_{i/o}$  proteins, we sought to develop a novel  
82 approach with sufficient sensitivity to study oGPCR pharmacology.

83 We generated a library of GPCRs that comprises the entire class C GPCR family and a  
84 subset of class A members including a total of 19 oGPCRs for testing with several luciferase  
85 reporter systems activated in response to G proteins stimulation. Luciferase reporters are  
86 characterized by high sensitivity and a wide dynamic range, allowing the detection of even minor  
87 levels of G protein-initiated signaling pathways (Cheng et al., 2010). These systems encode either  
88 firefly luciferase or nanoluc under the control of inducible promoters downstream of the main G  
89 protein-promoted signaling cascades.  $G_{\alpha}$  proteins are classified into four major families:  $G_s$ ,  $G_q$ ,  
90  $G_{12/13}$ , and  $G_{i/o}$ . In detail, activation of  $G_s$  family members ( $G_{s/olf}$ ) stimulates adenylyl cyclase to  
91 produce cAMP that triggers downstream signaling events which activate the cAMP response  
92 element (CRE). A primary effector of heterotrimeric  $G_q$  family members ( $G_{q/11/14/15}$ ) is  
93 phospholipase  $C\beta$  (PLC $\beta$ ) that catalyzes the formation of second messengers inositol 1,4,5-  
94 trisphosphate and diacylglycerol leading to the activation of the Nuclear Factor of Activated T-  
95 cells (NFAT) promoter. The canonical downstream target of the heterotrimeric  $G_{12/13}$  proteins is a  
96 group of Rho guanine nucleotide exchange factors (RhoGEFs) that activate the Ras-family small  
97 GTPase RhoA.  $G_{12/13}$  activation can be detected by luciferase reporters using promoters  
98 comprising a serum response element (SRE), or serum response factor response element (SRF-  
99 RE), with the last one designed to respond to SRF-dependent and ternary complex factor (TCF)-  
100 independent pathways (Cheng et al., 2010). Conversely, detection of active G proteins belonging  
101 to the  $G_{i/o}$  family ( $G_{i1/i2/i3/o/z/t}$ ) is more complicated and elusive. In fact, the main effect of  $G_{i/o}$   
102 stimulation consists in the inhibition of adenylyl cyclase, leading to a reduction of the cAMP  
103 production. Changes in cAMP levels can be readily detected after agonist-stimulation of  $G_{i/o}$ -  
104 coupled GPCRs, however, determining the constitutive activity of such receptors has proven  
105 challenging. Moreover, according to the GPCR database (Flock et al., 2017; Pandey-Szekeres et  
106 al., 2018) ([https://gpcrdb.org/signprot/statistics\\_venn](https://gpcrdb.org/signprot/statistics_venn)), 158 out of 247 ligand-activated GPCRs  
107 (64%) can activate members of the  $G_{i/o}$  protein family, with half of them, 79 out of 247 (32%),  
108 showing exclusive coupling to  $G_{i/o}$ . Considering the likely large number of  $G_{i/o}$ -coupled receptors  
109 among oGPCRs, research in this field is in desperate need of innovative sensitive tools.

110 To overcome this issue, we took advantage of previously developed G protein chimeras  
111 (Ballister, Rodgers, Martial, & Lucas, 2018; Conklin, Farfel, Lustig, Julius, & Bourne, 1993; Inoue  
112 et al., 2019), and generated novel G protein chimeras to expand the GPCR toolkit. Swapping the  
113 C-terminal strand of amino acids of any G protein with those of  $G_{i/o}$  family members enables

114 GPCRs that preferentially couple to  $G_{i/o}$  to trigger alternative downstream signaling events  
115 (Ahmad, Wojciech, & Jockers, 2015; Ballister et al., 2018; Conklin et al., 1993; Coward, Chan,  
116 Wada, Humphries, & Conklin, 1999; Inoue et al., 2019). Exploiting such property, we rerouted  
117 pathways initiated by the constitutive activation of  $G_{i/o}$ -coupled receptors to different downstream  
118 signaling outcomes which are more readily measurable. Herein, we tested 8 G protein chimeras  
119 against a set of 8 well-characterized  $G_{i/o}$ -coupled receptors for a total of 64 combinations to  
120 identify the most suitable ones for analysis of constitutive activity across our oGPCR library.  
121 Applying this strategy we successfully identified 8 oGPCRs that show significant basal activation  
122 of  $G_{i/o}$  proteins. We finally validated these results by measuring the inhibition of forskolin-induced  
123 cAMP production by an oGPCR showing high  $G_{i/o}$  constitutive activity, GPR156.

124

## 125 **2. METHODS**

### 126 **2.1 Cell cultures and transfections.**

127 HEK293T/17 cells were cultured at 37°C and 5% CO<sub>2</sub> in Dulbecco's Modified Eagle's Medium  
128 (DMEM; Gibco, 10567-014) supplemented with 10% fetal bovine serum (FBS; Biowest, S1520),  
129 Minimum Eagle's Medium (MEM) non-essential amino acids (Gibco, 11140-050), and antibiotics  
130 (100 units/ml penicillin and 100 µg/ml streptomycin; Gibco, 15140-122). HEK293 cells were  
131 seeded in 6-well plates in medium without antibiotics at a density of  $1 \times 10^6$  cells/well. After 4  
132 hours, cells were transfected using linear 25 kDa polyethylenimine (PEI) (VWR; AAA43896) at a  
133 1:3 ratio between total µg of DNA plasmid (2.5 µg) and µl of PEI (7.5 µl). A pcDNA3.1 empty  
134 vector was used to normalize the amount of transfected DNA. For western blot and BRET assays,  
135 cells were collected 24 hours after transfection. For CRE and NFAT luciferase reporter assays,  
136 cells were incubated overnight and then serum-starved in Opti-MEM Reduced Serum Media  
137 (Gibco, 11058-021) for 4 hours before collection. For SRE and SRF-RE luciferase reporter  
138 assays, cells were incubated overnight and then serum-starved in Opti-MEM for 24 hours before  
139 collection.

### 140 **2.2 DNA constructs and cloning.**

141 Details about the DNA constructs used in this paper are listed in the Supplementary table 1.  
142 Plasmids encoding GPR158, GPR179, ADRA2A, LPAR2, CHRM1, GRM1, GRM2, GRM3,  
143 GRM4, GRM6, GRM7, GRM8, GABBR1, GABBR2, masGRK3CT-Nluc,  $G\alpha_{i1}$ ,  $G\alpha_{i3}$ ,  $G\alpha_{oA}$ , and  $G\alpha_z$   
144 were generous gifts from Dr. Kirill Martemyanov (The Scripps Research Institute, FL). The  
145 plasmid encoding the human GRM5a was a kind gift from Dr. Paul Kammermeier (University of

146 Rochester, NY). G $\beta$ 1-Venus156-239 and G $\gamma$ 2-Venus1-155 were generous gifts from Dr. Nevin  
147 Lambert (Augusta University, GA) (Hollins, Kuravi, Digby, & Lambert, 2009). Plasmids encoding  
148 the cAMP sensor (pGloSensor-22F) and the following luciferase reporters were purchased from  
149 Promega: CRE-luc2, CRE-Nluc, NFAT-luc2, NFAT-Nluc, SRE-luc2, and SRF-RE-luc2. The  
150 plasmid encoding for the renilla luciferase under control of the constitutively active thymidine  
151 kinase promoter (pRL-tk) was a kind gift from Dr. Mark Ginsberg (University of California San  
152 Diego, CA). Plasmids encoding the following GPCRs were obtained from cDNA Resource Center  
153 ([www.cdna.org](http://www.cdna.org)): ADRB2, HTR1A, HTR2A, HTR4, and DRD1. The following cDNA clones from  
154 the Mammalian Gene Collection (MGC) encoding for full-length GPCR sequences required to  
155 further subcloning were purchased from Horizon Discovery: GPR19, GPR37, GPR85, GPR137,  
156 GPR137b, GPR162, GPR176, GPR180, CaSR, GPR156, GPRC5A, GPRC5B, GPRC5C, and  
157 GPRC6A. Codon optimized sequences for the following oGPCRs used to further subcloning were  
158 a kind gift from Dr. Bryan Roth (University of North Carolina, NC) (Kroeze et al., 2015): GPR22  
159 (Addgene plasmid #66346), GPR88 (Addgene plasmid #66380), GPR151 (Addgene plasmid  
160 #66327). The plasmids encoding the following G $_q$ -derived chimeras were a kind gift from Dr. Bruce  
161 Conklin (University of California San Francisco, CA) (Conklin et al., 1993): qo5 (Addgene plasmid  
162 #24500), qi<sub>1</sub>5 (Addgene plasmid #24501), qz5 (Addgene plasmid #25867). The plasmids  
163 encoding the following G $_s$ -derived chimeras were a kind gift from Dr. Robert Lucas (University of  
164 Manchester, UK) (Ballister et al., 2018): Gsz (Addgene plasmid #109355), Gso (Cys) (Addgene  
165 plasmid #109375), Gsi (Cys) (Addgene plasmid #109373). The plasmids encoding the following  
166 GPCRs were a kind gift from Dr. Erik Procko (University of Illinois at Urbana, IL) (Park et al.,  
167 2019): HLA-cMyc-EcopT1R1 (Addgene plasmid #113962), HLA-Flag-natT1R3 (Addgene plasmid  
168 #113950), HA-Flag-natT1R2 (Addgene plasmid #113944). The codon optimized sequence for  
169 human GPRC5D expression in mammalian cells was synthesized by Integrated DNA  
170 Technologies as a gene block and inserted into a pcDNA3.1 vector including a C-terminal HA-tag  
171 using In-Fusion HD Cloning technology (Clontech). The full-length sequences of all the orphan  
172 GPCRs (except GPR158 and GPR179) were subcloned into a pcDNA3.1 vector for mammalian  
173 expression and a C-terminal HA-tag (YPYDVPDYA) was added using In-Fusion HD Cloning  
174 technology (Clontech). A plasmid encoding the G protein chimera G $_q$ G $_{i3}$  bearing the core of  
175 human G $\alpha_q$  and the last 4 amino acid of G $\alpha_{i3}$  was generated by primer mutagenesis and In-Fusion  
176 HD Cloning (Clontech) in a pcDNA3.1 vector. All constructs were verified by Sanger sequencing.

### 177 **2.3 Western blot.**

178 For Western blotting analysis, transfected cells were harvested and lysed by sonication in ice-  
179 cold immunoprecipitation buffer (300 mM NaCl, 50 mM Tris-HCl, pH 7.4, 1% Triton X-100, and

180 complete protease inhibitor mixture). Lysates were cleared by centrifugation at 14,000 rpm for 15  
181 min, and the supernatants were diluted in SDS sample buffer (final concentrations: 50 mM Tris-  
182 HCl pH 6.8, 1% SDS, 10% glycerol, 143 mM 2-mercaptoethanol, and 0.08 mg/ml bromophenol  
183 blue). 10  $\mu$ l of each protein sample were loaded and analyzed by SDS-PAGE. Orphan GPCR  
184 expression was detected using rat anti-HA tag (clone 3F10) antibodies (Sigma-Aldrich;  
185 11867423001) or rabbit anti-myc tag antibodies (GenScript; A00172).

#### 186 **2.4 Luciferase reporter assays.**

187 HEK293T/17 cells were plated at a density of  $1 \times 10^6$  cells/well in 6-well plates in antibiotic-free  
188 medium and transfected as described above. 2.5  $\mu$ g of total DNA plasmids were transfected  
189 according to the following ratio: 0.97  $\mu$ g of pRL-tk plasmid expressing renilla luciferase under  
190 control of the constitutive thymidine kinase promoter; 0.14  $\mu$ g of luciferase reporter (NFAT-Fluc,  
191 CRE-Fluc, SRE-Fluc, and SRF-RE-Fluc for screening of  $G_q$ ,  $G_s$ , and  $G_{12/13}$  activation; NFAT-Nluc  
192 and CRE-Nluc for screening of  $G_{i/o}$  activation); 1.11  $\mu$ g of GPCR; and only in experiments  
193 screening  $G_{i/o}$  activation, 0.28  $\mu$ g of G protein chimeras ( $G_qG_{i1}$ ,  $G_qG_{i1-9}$ ,  $G_qG_{i3}$ ,  $G_qG_o$ ,  $G_qG_z$ ,  $G_sG_{i1}$ ,  
194  $G_sG_o$ , or  $G_sG_z$ ). pcDNA3.1 was used to normalize the amount of transfected DNA. For CRE and  
195 NFAT luciferase reporter assays, cells were incubated overnight and then serum-starved in Opti-  
196 MEM for 4 hours before collection. For SRE and SRF-RE luciferase reporter assays, cells were  
197 incubated overnight and then serum-starved in Opti-MEM for 24 hours before collection.  
198 Transfected cells were harvested, centrifuged for 5 minutes at 500g, and resuspended in 500  $\mu$ l  
199 of PBS containing 0.5 mM  $MgCl_2$  and 0.1% glucose. 50  $\mu$ l of cells were incubated in 96-well flat-  
200 bottomed white microplates (Greiner Bio-One) with 50  $\mu$ l of luciferase substrate according to  
201 manufacturers' instructions: furimazine (Promega NanoGlo; N1120) for nanoluc, e-coelenterazine  
202 (Nanolight; 355) for renilla luciferase, and luciferin (Promega BrightGlo; E2610) for firefly  
203 luciferase. Luciferase levels were quantified using a POLARstar Omega microplate reader (BMG  
204 Labtech). Renilla luciferase expression was used to normalize the signal in order to compensate  
205 for variability due to transfection efficiency and number of cells.

#### 206 **2.5 Bioluminescence Resonance Energy Transfer (BRET) assays.**

207 Measurements of ADRA2A activation by norepinephrine in live cells by measurement of BRET  
208 between Venus-G $\beta$ 1 $\gamma$ 2 and masGRK3CT-Nluc was performed as described previously (Masuho,  
209 Martemyanov, & Lambert, 2015). 2.5  $\mu$ g of total DNA plasmids were transfected according to the  
210 following ratio: 0.21  $\mu$ g of G $\beta$ 1-Venus156-239; 0.21  $\mu$ g of Gy2-Venus1-155; 0.21  $\mu$ g of  
211 masGRK3CT-Nluc; 0.42  $\mu$ g of G $\alpha_{i/o}$  proteins or  $G_q$ -derived chimeras ( $G\alpha_{i1}$ ,  $G\alpha_{i3}$ ,  $G\alpha_o$ ,  $G\alpha_z$ ,  $G_qG_{i1}$ ,  
212  $G_qG_{i1-9}$ ,  $G_qG_{i3}$ ,  $G_qG_o$ ,  $G_qG_z$ ) or 1.25  $\mu$ g of G $\alpha_s$ -derived chimeras ( $G_sG_i$ ,  $G_sG_o$ , or  $G_sG_z$ ); and 0.21

213 µg of ADRA2A. Empty vector pcDNA3.1 was used to normalize the amount of transfected DNA.  
214 18 hours after transfection, HEK293T cells were washed once with phosphate-buffered saline  
215 (PBS). Cells were then mechanically harvested using a gentle stream of PBS, centrifuged at 500  
216 g for 5 minutes, and resuspended in 500 µl of PBS containing 0.5 mM MgCl<sub>2</sub> and 0.1% glucose.  
217 25 µl of resuspend cells were distributed in 96-well flat-bottomed white microplates (Greiner Bio-  
218 One). The nanoluc substrate furimazine (N1120) was purchased from Promega and used  
219 according to the manufacturer's instructions. BRET measurements were obtained using a  
220 POLARstar Omega microplate reader (BMG Labtech) which permits detection of two emissions  
221 simultaneously with the highest possible resolution of 20 ms per data point. All measurements  
222 were performed at room temperature. The BRET signal was determined by calculating the ratio  
223 of the light emitted by Venus-Gβ1γ2 (collected using the emission filter 535/30) to the light emitted  
224 by masGRK3CT-Nluc (475/30). The average baseline value (basal BRET ratio) recorded for 5  
225 seconds before agonist application was subtracted from the BRET signal to obtain the ΔBRET  
226 ratio.

## 227 **2.6 cAMP assay.**

228 HEK293T cells were transfected with an equal ratio of indicated GPCR plasmid and  
229 pGloSensor™-22F cAMP plasmid (Promega). 18 hours post-transfection, cells were detached  
230 with 1 ml of PBS, centrifuged at 500 g for 5 minutes, and resuspended in 300 µl of PBS containing  
231 0.5 mM MgCl<sub>2</sub> and 0.1% glucose. 40 µl of the cell suspension were transferred to each well of 96-  
232 well plates containing 10 µl of 5X GloSensor cAMP Reagent (Promega) prepared according to  
233 the manufacturer's instruction. Cells were then incubated at 37°C for 2 hours and let cool down  
234 to room temperature for 10 minutes. Luminescence was monitored every 30 seconds using a  
235 POLARstar Omega microplate reader (BMG Labtech) at room temperature. After 3 minutes,  
236 forskolin (Tocris; 1099) was added to the cells at a final concentration of 0.5 µM.

## 237 **2.7 Statistical analysis.**

238 Analyses were performed using GraphPad Prism 9 software and number of biological and  
239 technical replicates are described in the figure legends. Data in figure 4 were analyzed by  
240 normalizing the nanoluc/renilla luciferase ratio by control cells not transfected with the G protein  
241 chimeras. One-way ANOVA with Dunnett's multiple comparisons test was performed comparing  
242 the signal obtained with each oGPCRs against control cells not expressing GPCRs.

243

## 244 **3. RESULTS**



### 245 **3.1 Screening of GPCR constitutive activity using luciferase reporter assays.**

246 Taking advantage of a plasmid cDNA library encoding the entire 22 class C GPCRs, including 8  
247 oGPCRs, and a subset of 19 class A GPCRs, including 11 oGPCRs, we systematically tested  
248 their constitutive activity using several luciferase reporter assays and setting an arbitrary threshold  
249 of 3 fold-increase for positive signals (Figure 1). We first screened the library for  $G_q$  activation by  
250 co-transfecting HEK293T cells with each GPCR and a NFAT-RE luciferase reporter (Figure 1a).  
251 As expected, the positive controls serotonin 2A receptor (HTR2A), muscarinic receptor 1  
252 (CHRM1), and the metabotropic glutamate receptors 1 and 5 (GRM1 and GRM5) showed the  
253 highest signal compared to control cells expressing only the luciferase reporter. None of the  
254 oGPCRs tested showed any constitutive activation of  $G_q$ -dependent signaling pathways (Figure  
255 1a). Similarly, using a CRE reporter assay for  $G_s$  activation, we detected the constitutive activity  
256 of  $\beta 2$  adrenergic receptor (ADRB2), serotonin receptor 4 (HTR4), and dopamine receptor D1  
257 (DRD1) (Figure 1b). Interestingly, some  $G_q$ -coupled receptors also triggered the expression of  
258 luciferase activating the CRE reporter, while all the oGPCRs showed levels of activation  
259 comparable to those of the control not expressing GPCRs (Figure 1b). Using the same approach  
260 with two additional luciferase reporters SRE and SRF-RE, we detected the constitutive activity of  
261 the lysophosphatidic acid receptor 2 (LPAR2) downstream of  $G_{12/13}$  (Figure 1c-d). Again, no  
262 constitutive luciferase expression by oGPCRs was detected (Figure 1c-d). Overall, these  
263 experiments revealed that luciferase reporters are sensitive enough to detect GPCR activity in  
264 the absence of ligand application for some GPCRs; however, none of the 19 oGPCRs tested  
265 showed any constitutive activation of  $G_q$ ,  $G_s$ , or  $G_{12/13}$  signaling pathways.

### 266 **3.2 G protein chimeras are valuable tools to detect constitutive activity of $G_{i/o}$ -coupled** 267 **receptors.**

268 After exploring our GPCR library for the activation of signaling pathways downstream of  $G_s$ ,  $G_q$ ,  
269 and  $G_{12/13}$ , we focused on  $G_{i/o}$  signaling. In principle, the CRE luciferase reporter could be used  
270 to detect activation of  $G_{i/o}$ -coupled GPCRs as a reduction in cAMP levels, however its use is  
271 limited by a low dynamic range. This especially applies to measurements of GPCR constitutive  
272 activity, as they are intrinsically small. Therefore, to obtain a reliable quantification of constitutive  
273 activation of  $G_{i/o}$  signaling, we tested several G protein chimeras based on  $G_q$  or  $G_s$  core protein  
274 and bearing the C-terminus of either  $G_{i1}$ ,  $G_{i3}$ ,  $G_o$ , or  $G_z$  (Figure 2a). The last few amino acids in  
275 the  $G\alpha$  protein C-terminus define most of the GPCR coupling selectivity (Ballister et al., 2018;  
276 Conklin et al., 1993; Inoue et al., 2019). However, the coupling efficiency of G protein chimeras  
277 is variable and depends on the GPCR analyzed (Ballister et al., 2018; Conklin et al., 1993; Inoue  
278 et al., 2019). Thus, we tested 5 chimeras based on a  $G_q$  core and 3 chimeras based on a  $G_s$  core

279 for their ability to stimulate NFAT or CRE luciferase reporters, respectively. As a control, we first  
280 quantified the amount of luciferase expressed in cells where each chimera was co-transfected  
281 with the associated luciferase reporter but without GPCR overexpression. We reasoned that the  
282 difference in luciferase expression obtained comparing cells expressing the reporter with or  
283 without expression of the G protein chimeras could represent an index of reporter activation by  
284 endogenously expressed  $G_{i/o}$ -coupled receptors. As a positive control, we co-transfected GRM2  
285 because of its reported high constitutive activity (Doornbos et al., 2018) (Figure 2b-c). We found  
286 that expression of  $G_q$ -based chimeras only produced a negligible amount of NFAT reporter  
287 induction (0.1-fold increase on average) (Figure 2b), while we observed an average of 83-fold  
288 increase in CRE-induced luciferase expression using the  $G_s$ -based chimeras (Figure 2c). As  
289 expected, expression of GRM2 significantly induced the luciferase expression with all of the  
290 chimeras tested (Figure 2b-c). The fold-change observed normalizing the GRM2 constitutive  
291 activity over the no-GPCR control, revealed comparable levels of activation between  $G_q$  and  $G_s$   
292 chimeras. Interestingly, the  $G_qG_{i3}$  chimera showed a  $29.3 \pm 3.5$  fold-increase, being the highest  
293 amplitude among all the chimeras, while both the  $G_qG_z$  and the  $G_sG_z$  chimeras showed only a  $4.7$   
294  $\pm 0.6$  and  $3.8 \pm 0.4$  fold-increase (Figure 2b-c). To explore the efficiency of activation of these G  
295 protein chimeras, we then quantified the constitutive activity of eight GPCRs that are known to  
296 primarily couple to  $G_{i/o}$  (Flock et al., 2017; Pandey-Szekeres et al., 2018): class C GRM2, GRM3,  
297 GRM4, GRM6, GRM7, GRM8, and class A ADRA2A and HTR1A (Figure 2d). Assuming an  
298 arbitrary threshold of 3 fold-increase as a positive signal, our data show that some GPCR  
299 constitutive activity can be detected with the majority of the chimeras (i.e. GRM2), while some  
300 GPCRs show levels of activation above the threshold only if co-transfected with  $G_sG_{i1}$  or  $G_sG_o$   
301 chimeras (i.e. GRM7 and GRM8). According to earlier reports, the signal amplitude is GPCR-  
302 dependent (Conklin et al., 1993), and here we show it is undetectable for a subset of GPCR (i.e.  
303 ADRA2A). We next asked if the absence of signal for ADRA2A could be due to a lack of  
304 constitutive activity or to the expression of a non-functional receptor. Using a Bioluminescence  
305 Resonance Energy Transfer (BRET) assay we tested the ligand activation of the G protein  
306 chimeras by ADRA2A (Figure 3a). Here, we activated the ADRA2A receptor with the endogenous  
307 agonist norepinephrine at a concentration of 1  $\mu$ M. We compared the  $\Delta$ BRET ratio obtained using  
308 G protein chimeras with those obtained with wild type  $G_{i1}$ ,  $G_{i3}$ ,  $G_o$ , and  $G_z$  proteins (Figure 3b-d).  
309 Although the amplitude of the BRET signal generated by the G protein chimeras was smaller  
310 compared to the signal produced by wild type G protein, our data show that ADRA2A can indeed  
311 activate every tested chimera. Overall, we provide evidence that ADRA2A lacks detectable levels

312 of constitutive activity. Likewise, we expect that the constitutive activity of some of the oGPCRs  
313 in our library will also be undetectable.

### 314 **3.3. Identification of oGPCRs that signal through $G_{i/o}$ .**

315 Agonist-activation of a subset of  $G_{i/o}$  coupled receptors, M4R, D2R,  $\alpha 2AAR$ , and A1R, using G  
316 protein chimeras was previously reported to be strongly dependent on both the  $G_{i/o}$  protein core  
317 and the  $G_{i/o}$  C-terminus (Okashah et al., 2019). However, among the possible combinations of G  
318 protein cores and C-termini, it was established that chimeras based on  $G_s$  could be triggered by  
319  $G_{i/o}$  coupled receptors more easily than chimeras bearing the core of  $G_q$  or  $G_{12/13}$  (Okashah et al.,  
320 2019). Our data on 8 control GPCRs suggest similar preference pattern, with  $G_s$  chimeras being  
321 more promiscuous than  $G_q$  chimeras (Figure 2d). We thus screened our oGPCR library for  
322 constitutive activation of  $G_sG_{i1}$  and  $G_sG_o$  chimeras normalizing the luciferase signal to that  
323 obtained in cells transfected only with the luciferase reporters but no G protein chimeras (Figure  
324 4a-b). Excitingly, this optimized assay indicated that 8 of the 19 oGPCRs examined can indeed  
325 activate  $G_{i/o}$  proteins. Specifically, we confirmed previously identified  $G_{i/o}$  coupling for the orphan  
326 receptors GPR22 (Adams et al., 2008), GPR88 (Dzierba et al., 2015; Jin et al., 2014) and  
327 GPRC6A (Pi, Parrill, & Quarles, 2010), even though some reports failed to reproduce  $G_{i/o}$  coupling  
328 for GPRC6A (Jacobsen et al., 2013). Moreover, we revealed previously unreported robust and  
329 significant constitutive activity for GPR156 ( $8.94 \pm 0.40$  fold increase over control using the  $G_sG_{i1}$   
330 chimera), GPR137b ( $4.05 \pm 0.45$ ), GPR158 ( $4.87 \pm 0.32$ ), GPR179 ( $7.97 \pm 0.55$ ), and GPRC5D  
331 ( $3.61 \pm 0.17$ ) (Figure 4a-b).

332 The lack of signal obtained transfecting several oGPCRs with any of the tested luciferase  
333 reporters may be due to a variety of factors. For example, we demonstrated that ADRA2A receptor  
334 was functional in activating wild type or chimeric G proteins (Figure 3b-d), but did not produce a  
335 detectable basal G protein signaling (Figure 2d) pointing at a very low level of constitutive activity.  
336 Alternatively, the absence of signal could depend on DNA constructs that do not express  
337 adequate levels of GPCRs. To test this possibility, we analyzed the expression of our oGPCR  
338 library at the protein level by western blot using antibodies directed against C-terminus HA-tag  
339 (Figure 4c-d) or myc-tag (Figure 4e). Immunoblots revealed that the expression levels of GPR85  
340 and GPR137 were below detectable threshold, thus providing a possible explanation for their lack  
341 of signal (Figure 4c).

### 342 **3.4. Validation of GPR156 constitutive activation of $G_{i/o}$ proteins.**

343 Adenylate cyclase represents one of the main intracellular effectors for both  $G_s$  and  $G_i$  protein  
344 signaling, with  $G_s$  stimulating cAMP production and  $G_i$  inhibiting it. To validate the results obtained

345 measuring  $G_{i/o}$  constitutive activation by oGPCRs shown in figure 4, we quantified the reduction  
346 in cAMP levels induced by treatment with the adenylate cyclase stimulant forskolin in cells  
347 overexpressing GPR156, GRM2 or GPRC5B. Using a co-transfected cAMP sensor, we were able  
348 to obtain real time measurements of cAMP changes (Figure 5a). As expected, we found that  
349 forskolin stimulation of cAMP levels was not affected by overexpression of GPRC5B ( $107.8 \pm$   
350  $6.5\%$  of CNT;  $p = 0.622$ ); while overexpression of the positive control GRM2 ( $54.6 \pm 4.7\%$  of CNT)  
351 or the orphan receptor GPR156 ( $65.7 \pm 5.2\%$  of CNT) significantly blunted the effect of forskolin  
352 (Figure 5a-b). These results confirmed the earlier identified  $G_{i/o}$  coupling and high constitutive  
353 activity for GPR156, as well as the lack of  $G_{i/o}$  signaling for GPRC5B.

354

#### 355 4. DISCUSSION

356 The unique properties of each GPCR together with the plethora of signaling cascades  
357 activated makes the development of tailor-made assays a prerequisite for future attempts at  
358 profiling oGPCR signaling. Many efforts have been made to create a universal platform for high-  
359 throughput screening of GPCR signaling that is independent of G protein coupling (Inoue et al.,  
360 2012; Kroeze et al., 2015). For example, the use of quantitative techniques to measure  $\beta$ -arrestin  
361 recruitment as a general readout of GPCR activation led to the identification of a number of  
362 compounds within a library of 446 molecules acting as agonists or antagonists for class A  
363 oGPCRs (Kroeze et al., 2015). However, despite the ability of class C GPCR members to recruit  
364  $\beta$ -arrestins (Iacovelli, Felicioni, Nistico, Nicoletti, & De Blasi, 2014; Mos, Jacobsen, Foster, &  
365 Brauner-Osborne, 2019; Mundell, Matharu, Pula, Roberts, & Kelly, 2001; Stoppel et al., 2017),  
366 attempts to use this approach to deorphanize this subfamily of oGPCRs were unsuccessful  
367 (Kroeze et al., 2015). Similarly, the use of cell-based assays expressing G protein chimeras in G  
368 protein knock out cell lines to measure ligand-activated GPCR signaling has recently found a  
369 number of applications (Inoue et al., 2019; Okashah et al., 2019). Overall, we expect that a single  
370 readout would never be sufficient to detect the activation of every oGPCR without possibly  
371 omitting important ligand-receptor pairs. In fact, successful screening efforts will probably need to  
372 include multiple alternative readouts. A systematic parallel analysis of GPCR constitutive activity  
373 represents a powerful strategy to begin understanding the cell signaling pathways modulated by  
374 oGPCRs. Using a novel approach combining luciferase reporter assays with G protein chimeras,  
375 here we detected  $G_{i/o}$  protein activation by several oGPCRs in absence of ligand stimulation,  
376 thereby providing the first evidence for G protein coupling-preference for multiple oGPCRs. This  
377 information is crucial in the deorphanization process, as it provides a novel readout in designing

378 platforms to test the activation of oGPCRs allowing for the analysis of libraries of synthetic or  
379 endogenous compounds.

380 In the present study, we did not find evidence of  $G_s$ ,  $G_q$ , or  $G_{12/13}$  coupling for any of the  
381 19 oGPCRs analyzed, nevertheless, we confirmed  $G_{i/o}$  coupling for GPR22, GPR88, and  
382 GPRC6A. Strikingly, we observed previously unappreciated  $G_{i/o}$  constitutive activities for  
383 GPR137b, GPR156, GPR158, GPR179, and GPRC5D. GPR137b expression is restricted to  
384 heart, liver, kidney and brain, and it is one of the few GPCRs enriched at lysosomal membranes  
385 (Gan et al., 2019; Gao et al., 2012). Proteomics studies of lysosomal membranes also identified  
386 several G protein signaling elements including  $G\alpha_{i2}$ ,  $G\beta_1$ , and  $G\beta_2$  (Callahan, Bagshaw, &  
387 Mahuran, 2009). The functional consequences of activating  $G_{i/o}$  signaling responses at the  
388 lysosomal membrane remain to be characterized. The group of Pangalos suggested that the class  
389 C orphan GPR156 could possibly act as a third GABA<sub>B</sub> receptor subunit because of their  
390 significant sequence homology (Calver et al., 2003). However, functional assays failed to reveal  
391 any activation in response to treatments with GABA<sub>B</sub> receptor agonists in cells expressing  
392 GPR156 alone or co-expressing GPR156 with GABA<sub>B1</sub> or GABA<sub>B2</sub> receptors (Calver et al., 2003).  
393 Searching for alternative ligands, a calcium mobilization assay was used to screen a library of  
394 2500 endogenous GPCR agonists without success (Calver et al., 2003). The extremely high  
395 constitutive activity of GPR156 could result in a low dynamic range when performing functional  
396 screens and therefore limit the chances to identify possible agonists. At the same time, a high  
397 constitutive activity can be a useful tool for the identification of inverse agonists that represent  
398 attractive compounds for multiple pharmacotherapies (Berg & Clarke, 2018; Bond & Ijzerman,  
399 2006; Chen et al., 2020). Our screening also revealed  $G_{i/o}$  constitutive activation for both GPR158  
400 and GPR179, highly homologous class C receptors. GPR158 is abundantly expressed in several  
401 neuronal populations in the brain where it regulates stress-induced depression (Orlandi et al.,  
402 2012; Orlandi, Sutton, Muntean, Song, & Martemyanov, 2019; Sutton et al., 2018). While,  
403 GPR179 is specifically expressed in the ON-bipolar neurons of the retina (Audo et al., 2012;  
404 Orlandi et al., 2012; Peachey et al., 2012). Point mutations in GPR179 gene were identified in  
405 patients with congenital stationary night blindness and further animal studies revealed its essential  
406 role in night vision (Audo et al., 2012; Peachey et al., 2012; Ray et al., 2014). At the molecular  
407 level, both GPR158 and GPR179 has been shown to interact and modulate the activity of a family  
408 of R7 Regulator of G protein signaling (R7-RGS) proteins (Orlandi et al., 2012). At the same time  
409 GPR179 acts as a scaffold for many components of the post-synaptic mGluR6-G<sub>o</sub>-TRPM1  
410 signaling complex (Orlandi, Cao, & Martemyanov, 2013). Moreover, their long extracellular N-  
411 termini have been shown to interact with extracellular matrix components to form trans-synaptic

412 complexes (Condomitti et al., 2018; Dunn, Orlandi, & Martemyanov, 2019; Orlandi et al., 2018).  
413 Our results here indicate that GPR158 and GPR179 can simultaneously activate G proteins of  
414 the  $G_{i/o}$  family while scaffolding R7-RGS proteins, which act as GTPase activating proteins (GAP)  
415 for a subset of  $G_{\alpha_{i/o}}$  family members to terminate the G protein signal. These complexes may be  
416 required for the timely inactivation of G proteins in response to extracellular events thus limiting  
417 the diffusion of activated G proteins to a restricted post-synaptic microenvironment. Alternatively,  
418 this receptor complex configuration may limit the diversity of G proteins activated by GPR158 and  
419 GPR179 to a subset of  $G_{\alpha_{i/o}}$  family members that are not a suitable substrate for R7-RGS proteins  
420 such as  $G_{\alpha_2}$ . Further studies are needed to investigate the molecular implications of G protein  
421 activation by GPR158 in the brain and GPR179 in the retina. The involvement of GPR158 in  
422 stress-induced depression makes it an ideal target for development of a novel antidepressants, a  
423 desperately needed class of pharmaceuticals. While GPR179 loss of function in congenital  
424 stationary night blindness, a debilitating disease without current available treatments, makes it  
425 also a relevant candidate for drug discovery ventures. Finally, we detected a previously  
426 unreported  $G_{i/o}$  coupling for GPRC5D, the last identified member of the class C retinoic acid-  
427 inducible receptor family (Brauner-Osborne et al., 2001). GPRC5D is mostly expressed in  
428 peripheral tissues and it has recently been associated with cancer (Atamaniuk et al., 2012; Smith  
429 et al., 2019). Specifically, its expression was found to be elevated on the surface of malignant  
430 cells involved in multiple myeloma, and it represents a viable target for chimeric antigen receptor  
431 (CAR) T cell immunotherapy of multiple myeloma (Kodama et al., 2019; Smith et al., 2019). The  
432 discovery of signaling pathways triggered by GPRC5D represents therefore an important step  
433 forward in the development of therapeutic treatments for white blood plasma cell cancer.

434 In summary, here we provided a new sensitive strategy to profile constitutive  $G_{i/o}$  protein  
435 coupling for understudied orphan GPCRs. This approach represents a fundamental advancement  
436 in the deorphanization process and will likely accelerate the search for novel GPCR ligands. By  
437 screening the entire class C GPCR family, we discovered or confirmed  $G_{i/o}$  coupling for 5 out of  
438 the 8 orphan members, and, similarly, we revealed 3  $G_{i/o}$  coupled receptors within a subset of  
439 class A oGPCRs. Several of these oGPCRs are associated with debilitating neuropsychiatric  
440 disorders or they are relevant for treatment of numerous cancers. Hence, improving our  
441 understanding of the biology of such receptors has clinical relevance and it is essential in the drug  
442 discovery process.

443

444

445 **Acknowledgments:** For providing essential cDNA constructs, we are sincerely grateful for Dr.  
446 Kirill A. Martemyanov (The Scripps Research Institute, Jupiter, FL), Dr. Paul J. Kammermeier  
447 (University of Rochester, NY), Dr. Nevin A. Lambert (Augusta University, GA), Dr. Mark H.  
448 Ginsberg (University of California San Diego, CA), Dr. Bryan L. Roth (University of North Carolina,  
449 NC), Dr. Bruce R. Conklin (University of California San Francisco, CA), Dr. Robert J. Lucas  
450 (University of Manchester, UK), and Dr. Erik Procko (University of Illinois at Urbana, IL). We also  
451 would like to thank Dr. Henry A. Dunn (The Scripps Research Institute, Jupiter, FL) for comments  
452 and fruitful discussions.

453 **Author Contributions:** Experimental investigation and data analysis, L.R.W. and C.O.;  
454 Conceptualization, C.O.; writing and editing—original draft preparation, C.O.; All authors have  
455 read and agreed to the published version of the manuscript.

456 **Funding:** This work was supported by start-up funding from the Department of Pharmacology  
457 and Physiology, University of Rochester School of Medicine and Dentistry.

458 **Conflicts of Interest:** The authors declare no conflict of interest.

459

## 460 References

- 461 Adams, J. W., Wang, J., Davis, J. R., Liaw, C., Gaidarov, I., Gatlin, J., . . . Connolly, D. (2008).  
462 Myocardial expression, signaling, and function of GPR22: a protective role for an orphan  
463 G protein-coupled receptor. *Am J Physiol Heart Circ Physiol*, *295*(2), H509-521.  
464 doi:10.1152/ajpheart.00368.2008
- 465 Ahmad, R., Wojciech, S., & Jockers, R. (2015). Hunting for the function of orphan GPCRs -  
466 beyond the search for the endogenous ligand. *Br J Pharmacol*, *172*(13), 3212-3228.  
467 doi:10.1111/bph.12942
- 468 Atamaniuk, J., Gleiss, A., Porpaczy, E., Kainz, B., Grunt, T. W., Raderer, M., . . . Gaiger, A. (2012).  
469 Overexpression of G protein-coupled receptor 5D in the bone marrow is associated with  
470 poor prognosis in patients with multiple myeloma. *Eur J Clin Invest*, *42*(9), 953-960.  
471 doi:10.1111/j.1365-2362.2012.02679.x
- 472 Audo, I., Bujakowska, K., Orhan, E., Poloschek, C. M., Defoort-Dhellemmes, S., Drumare, I., . . .  
473 Zeitz, C. (2012). Whole-exome sequencing identifies mutations in GPR179 leading to  
474 autosomal-recessive complete congenital stationary night blindness. *Am J Hum Genet*,  
475 *90*(2), 321-330. doi:10.1016/j.ajhg.2011.12.007
- 476 Ballister, E. R., Rodgers, J., Martial, F., & Lucas, R. J. (2018). A live cell assay of GPCR coupling  
477 allows identification of optogenetic tools for controlling Go and Gi signaling. *BMC Biol*,  
478 *16*(1), 10. doi:10.1186/s12915-017-0475-2
- 479 Berg, K. A., & Clarke, W. P. (2018). Making Sense of Pharmacology: Inverse Agonism and  
480 Functional Selectivity. *Int J Neuropsychopharmacol*, *21*(10), 962-977.  
481 doi:10.1093/ijnp/pyy071
- 482 Bond, R. A., & Ijzerman, A. P. (2006). Recent developments in constitutive receptor activity and  
483 inverse agonism, and their potential for GPCR drug discovery. *Trends Pharmacol Sci*,  
484 *27*(2), 92-96. doi:10.1016/j.tips.2005.12.007
- 485 Brauner-Osborne, H., Jensen, A. A., Sheppard, P. O., Brodin, B., Krogsgaard-Larsen, P., &  
486 O'Hara, P. (2001). Cloning and characterization of a human orphan family C G-protein  
487 coupled receptor GPRC5D. *Biochim Biophys Acta*, *1518*(3), 237-248. doi:10.1016/s0167-  
488 4781(01)00197-x
- 489 Callahan, J. W., Bagshaw, R. D., & Mahuran, D. J. (2009). The integral membrane of lysosomes:  
490 its proteins and their roles in disease. *J Proteomics*, *72*(1), 23-33.  
491 doi:10.1016/j.jprot.2008.11.007
- 492 Calver, A. R., Michalovich, D., Testa, T. T., Robbins, M. J., Jaillard, C., Hill, J., . . . Pangalos, M.  
493 N. (2003). Molecular cloning and characterisation of a novel GABAB-related G-protein  
494 coupled receptor. *Brain Res Mol Brain Res*, *110*(2), 305-317. doi:10.1016/s0169-  
495 328x(02)00662-9
- 496 Chen, Z., Chen, H., Zhang, Z., Ding, P., Yan, X., Li, Y., . . . Xu, J. (2020). Discovery of novel liver  
497 X receptor inverse agonists as lipogenesis inhibitors. *Eur J Med Chem*, *206*, 112793.  
498 doi:10.1016/j.ejmech.2020.112793
- 499 Cheng, Z., Garvin, D., Paguio, A., Stecha, P., Wood, K., & Fan, F. (2010). Luciferase Reporter  
500 Assay System for Deciphering GPCR Pathways. *Curr Chem Genomics*, *4*, 84-91.  
501 doi:10.2174/1875397301004010084
- 502 Condomitti, G., Wierda, K. D., Schroeder, A., Rubio, S. E., Vennekens, K. M., Orlandi, C., . . . de  
503 Wit, J. (2018). An Input-Specific Orphan Receptor GPR158-HSPG Interaction Organizes  
504 Hippocampal Mossy Fiber-CA3 Synapses. *Neuron*, *100*(1), 201-215 e209.  
505 doi:10.1016/j.neuron.2018.08.038
- 506 Conklin, B. R., Farfel, Z., Lustig, K. D., Julius, D., & Bourne, H. R. (1993). Substitution of three  
507 amino acids switches receptor specificity of Gq alpha to that of Gi alpha. *Nature*,  
508 *363*(6426), 274-276. doi:10.1038/363274a0

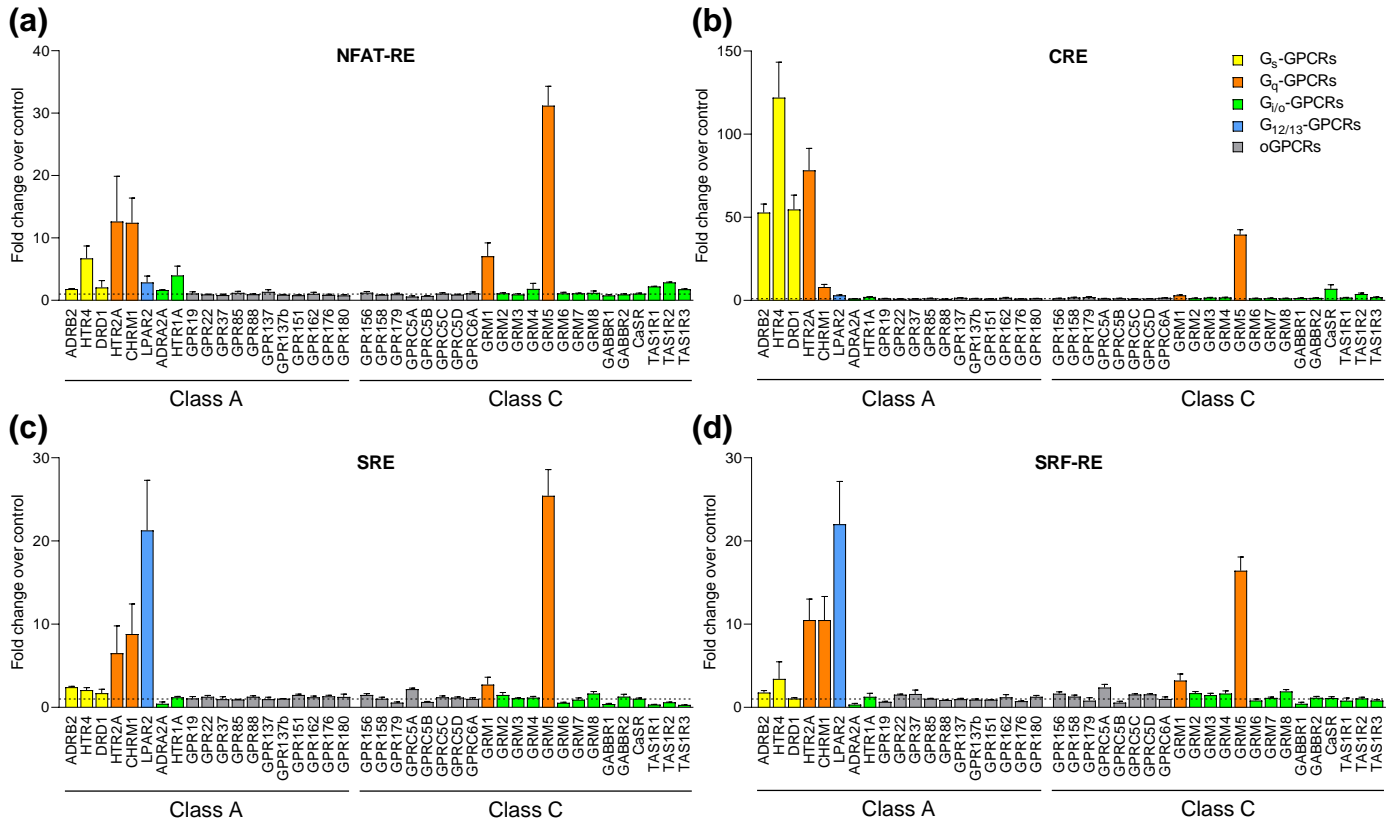


- 509 Corder, G., Doolen, S., Donahue, R. R., Winter, M. K., Jutras, B. L., He, Y., . . . Taylor, B. K.  
510 (2013). Constitutive mu-opioid receptor activity leads to long-term endogenous analgesia  
511 and dependence. *Science*, *341*(6152), 1394-1399. doi:10.1126/science.1239403
- 512 Coward, P., Chan, S. D., Wada, H. G., Humphries, G. M., & Conklin, B. R. (1999). Chimeric G  
513 proteins allow a high-throughput signaling assay of Gi-coupled receptors. *Anal Biochem*,  
514 *270*(2), 242-248. doi:10.1006/abio.1999.4061
- 515 Damian, M., Marie, J., Leyris, J. P., Fehrentz, J. A., Verdie, P., Martinez, J., . . . Mary, S. (2012).  
516 High constitutive activity is an intrinsic feature of ghrelin receptor protein: a study with a  
517 functional monomeric GHS-R1a receptor reconstituted in lipid discs. *J Biol Chem*, *287*(6),  
518 3630-3641. doi:10.1074/jbc.M111.288324
- 519 Doornbos, M. L. J., Van der Linden, I., Vereyken, L., Tresadern, G., AP, I. J., Lavreysen, H., &  
520 Heitman, L. H. (2018). Constitutive activity of the metabotropic glutamate receptor 2  
521 explored with a whole-cell label-free biosensor. *Biochem Pharmacol*, *152*, 201-210.  
522 doi:10.1016/j.bcp.2018.03.026
- 523 Dunn, H. A., Orlandi, C., & Martemyanov, K. A. (2019). Beyond the Ligand: Extracellular and  
524 Transcellular G Protein-Coupled Receptor Complexes in Physiology and Pharmacology.  
525 *Pharmacol Rev*, *71*(4), 503-519. doi:10.1124/pr.119.018044
- 526 Dzierba, C. D., Bi, Y., Dasgupta, B., Hartz, R. A., Ahuja, V., Cianchetta, G., . . . Macor, J. E.  
527 (2015). Design, synthesis, and evaluation of phenylglycinols and phenyl amines as  
528 agonists of GPR88. *Bioorg Med Chem Lett*, *25*(7), 1448-1452.  
529 doi:10.1016/j.bmcl.2015.01.036
- 530 Flock, T., Hauser, A. S., Lund, N., Gloriam, D. E., Balaji, S., & Babu, M. M. (2017). Selectivity  
531 determinants of GPCR-G-protein binding. *Nature*, *545*(7654), 317-322.  
532 doi:10.1038/nature22070
- 533 Gan, L., Seki, A., Shen, K., Iyer, H., Han, K., Hayer, A., . . . Meyer, T. (2019). The lysosomal  
534 GPCR-like protein GPR137B regulates Rag and mTORC1 localization and activity. *Nat*  
535 *Cell Biol*, *21*(5), 614-626. doi:10.1038/s41556-019-0321-6
- 536 Gao, J., Xia, L., Lu, M., Zhang, B., Chen, Y., Xu, R., & Wang, L. (2012). TM7SF1 (GPR137B): a  
537 novel lysosome integral membrane protein. *Mol Biol Rep*, *39*(9), 8883-8889.  
538 doi:10.1007/s11033-012-1755-0
- 539 Hauser, A. S., Attwood, M. M., Rask-Andersen, M., Schioth, H. B., & Gloriam, D. E. (2017). Trends  
540 in GPCR drug discovery: new agents, targets and indications. *Nat Rev Drug Discov*,  
541 *16*(12), 829-842. doi:10.1038/nrd.2017.178
- 542 Hollins, B., Kuravi, S., Digby, G. J., & Lambert, N. A. (2009). The c-terminus of GRK3 indicates  
543 rapid dissociation of G protein heterotrimers. *Cell Signal*, *21*(6), 1015-1021.  
544 doi:10.1016/j.cellsig.2009.02.017
- 545 Iacovelli, L., Felicioni, M., Nistico, R., Nicoletti, F., & De Blasi, A. (2014). Selective regulation of  
546 recombinantly expressed mGlu7 metabotropic glutamate receptors by G protein-coupled  
547 receptor kinases and arrestins. *Neuropharmacology*, *77*, 303-312.  
548 doi:10.1016/j.neuropharm.2013.10.013
- 549 Inoue, A., Ishiguro, J., Kitamura, H., Arima, N., Okutani, M., Shuto, A., . . . Aoki, J. (2012).  
550 TGFA $\alpha$  shedding assay: an accurate and versatile method for detecting GPCR  
551 activation. *Nat Methods*, *9*(10), 1021-1029. doi:10.1038/nmeth.2172
- 552 Inoue, A., Raimondi, F., Kadji, F. M. N., Singh, G., Kishi, T., Uwamizu, A., . . . Russell, R. B.  
553 (2019). Illuminating G-Protein-Coupling Selectivity of GPCRs. *Cell*, *177*(7), 1933-1947  
554 e1925. doi:10.1016/j.cell.2019.04.044
- 555 Jacobsen, S. E., Norskov-Lauritsen, L., Thomsen, A. R., Smajilovic, S., Wellendorph, P., Larsson,  
556 N. H., . . . Brauner-Osborne, H. (2013). Delineation of the GPRC6A receptor signaling  
557 pathways using a mammalian cell line stably expressing the receptor. *J Pharmacol Exp*  
558 *Ther*, *347*(2), 298-309. doi:10.1124/jpet.113.206276

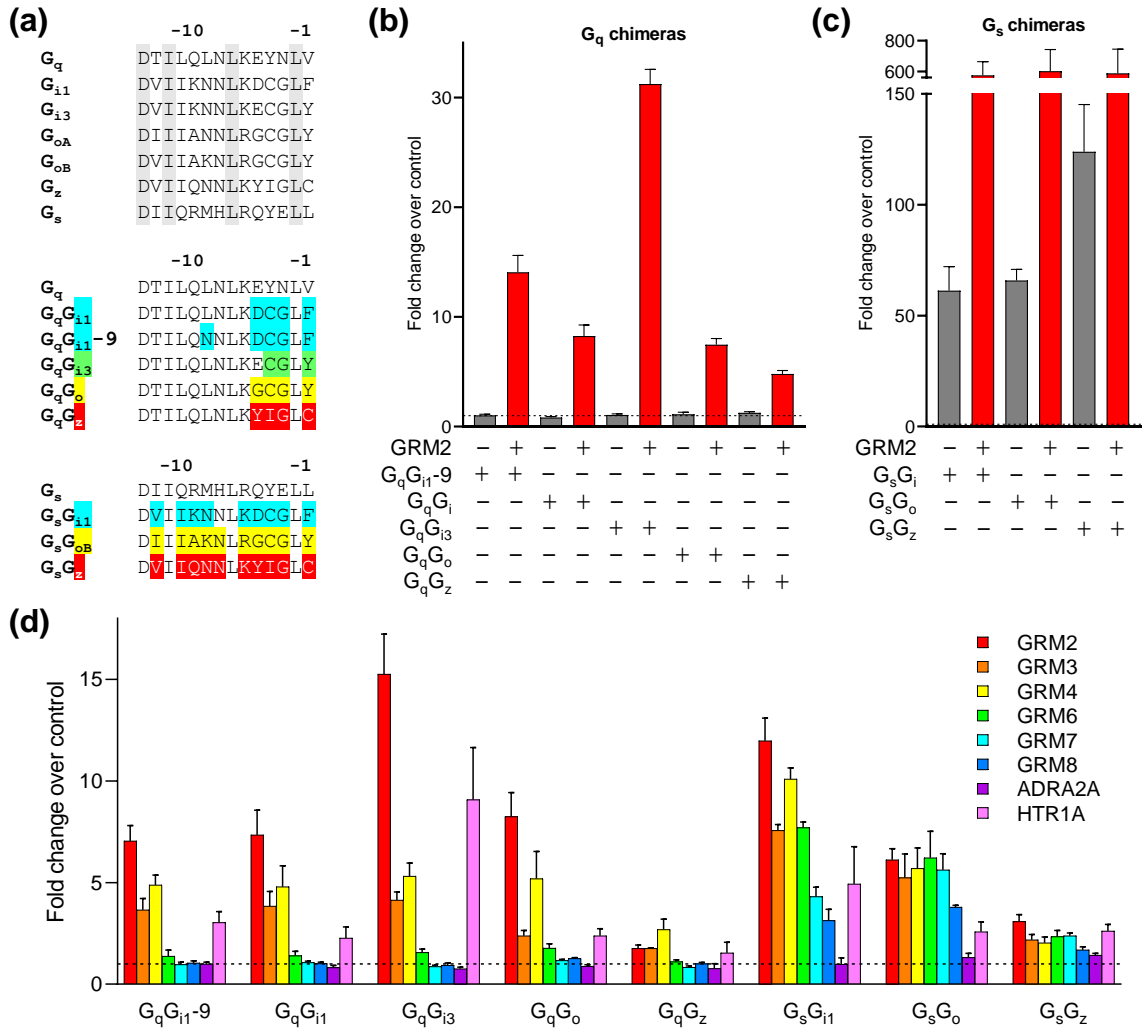
- 559 Jin, C., Decker, A. M., Huang, X. P., Gilmour, B. P., Blough, B. E., Roth, B. L., . . . Zhang, X. P.  
560 (2014). Synthesis, pharmacological characterization, and structure-activity relationship  
561 studies of small molecular agonists for the orphan GPR88 receptor. *ACS Chem Neurosci*,  
562 5(7), 576-587. doi:10.1021/cn500082p
- 563 Kodama, T., Kochi, Y., Nakai, W., Mizuno, H., Baba, T., Habu, K., . . . Akashi, K. (2019). Anti-  
564 GPRC5D/CD3 Bispecific T-Cell-Redirecting Antibody for the Treatment of Multiple  
565 Myeloma. *Mol Cancer Ther*, 18(9), 1555-1564. doi:10.1158/1535-7163.MCT-18-1216
- 566 Kroeze, W. K., Sassano, M. F., Huang, X. P., Lansu, K., McCorvy, J. D., Giguere, P. M., . . . Roth,  
567 B. L. (2015). PRESTO-Tango as an open-source resource for interrogation of the  
568 druggable human GPCRome. *Nat Struct Mol Biol*, 22(5), 362-369. doi:10.1038/nsmb.3014
- 569 Masuho, I., Martemyanov, K. A., & Lambert, N. A. (2015). Monitoring G Protein Activation in Cells  
570 with BRET. *Methods Mol Biol*, 1335, 107-113. doi:10.1007/978-1-4939-2914-6\_8
- 571 Mos, I., Jacobsen, S. E., Foster, S. R., & Brauner-Osborne, H. (2019). Calcium-Sensing Receptor  
572 Internalization Is beta-Arrestin-Dependent and Modulated by Allosteric Ligands. *Mol*  
573 *Pharmacol*, 96(4), 463-474. doi:10.1124/mol.119.116772
- 574 Mundell, S. J., Matharu, A. L., Pula, G., Roberts, P. J., & Kelly, E. (2001). Agonist-induced  
575 internalization of the metabotropic glutamate receptor 1a is arrestin- and dynamin-  
576 dependent. *J Neurochem*, 78(3), 546-551. doi:10.1046/j.1471-4159.2001.00421.x
- 577 Ngo, T., Coleman, J. L., & Smith, N. J. (2015). Using constitutive activity to define appropriate  
578 high-throughput screening assays for orphan g protein-coupled receptors. *Methods Mol*  
579 *Biol*, 1272, 91-106. doi:10.1007/978-1-4939-2336-6\_7
- 580 Okashah, N., Wan, Q., Ghosh, S., Sandhu, M., Inoue, A., Vaidehi, N., & Lambert, N. A. (2019).  
581 Variable G protein determinants of GPCR coupling selectivity. *Proc Natl Acad Sci U S A*,  
582 116(24), 12054-12059. doi:10.1073/pnas.1905993116
- 583 Orlandi, C., Cao, Y., & Martemyanov, K. A. (2013). Orphan receptor GPR179 forms  
584 macromolecular complexes with components of metabotropic signaling cascade in retina  
585 ON-bipolar neurons. *Invest Ophthalmol Vis Sci*, 54(10), 7153-7161. doi:10.1167/iovs.13-  
586 12907
- 587 Orlandi, C., Omori, Y., Wang, Y., Cao, Y., Ueno, A., Roux, M. J., . . . Martemyanov, K. A. (2018).  
588 Transsynaptic Binding of Orphan Receptor GPR179 to Dystroglycan-Pikachurin Complex  
589 Is Essential for the Synaptic Organization of Photoreceptors. *Cell Rep*, 25(1), 130-145  
590 e135. doi:10.1016/j.celrep.2018.08.068
- 591 Orlandi, C., Posokhova, E., Masuho, I., Ray, T. A., Hasan, N., Gregg, R. G., & Martemyanov, K.  
592 A. (2012). GPR158/179 regulate G protein signaling by controlling localization and activity  
593 of the RGS7 complexes. *J Cell Biol*, 197(6), 711-719. doi:10.1083/jcb.201202123
- 594 Orlandi, C., Sutton, L. P., Muntean, B. S., Song, C., & Martemyanov, K. A. (2019). Homeostatic  
595 cAMP regulation by the RGS7 complex controls depression-related behaviors.  
596 *Neuropsychopharmacology*, 44(3), 642-653. doi:10.1038/s41386-018-0238-y
- 597 Pandey-Szekeres, G., Munk, C., Tsonkov, T. M., Mordalski, S., Harpsoe, K., Hauser, A. S., . . .  
598 Gloriam, D. E. (2018). GPCRdb in 2018: adding GPCR structure models and ligands.  
599 *Nucleic Acids Res*, 46(D1), D440-D446. doi:10.1093/nar/gkx1109
- 600 Park, J., Selvam, B., Sanematsu, K., Shigemura, N., Shukla, D., & Procko, E. (2019). Structural  
601 architecture of a dimeric class C GPCR based on co-trafficking of sweet taste receptor  
602 subunits. *J Biol Chem*, 294(13), 4759-4774. doi:10.1074/jbc.RA118.006173
- 603 Peachey, N. S., Ray, T. A., Florijn, R., Rowe, L. B., Sjoerdsma, T., Contreras-Alcantara, S., . . .  
604 Gregg, R. G. (2012). GPR179 is required for depolarizing bipolar cell function and is  
605 mutated in autosomal-recessive complete congenital stationary night blindness. *Am J*  
606 *Hum Genet*, 90(2), 331-339. doi:10.1016/j.ajhg.2011.12.006
- 607 Pi, M., Parrill, A. L., & Quarles, L. D. (2010). GPRC6A mediates the non-genomic effects of  
608 steroids. *J Biol Chem*, 285(51), 39953-39964. doi:10.1074/jbc.M110.158063

- 609 Ray, T. A., Heath, K. M., Hasan, N., Noel, J. M., Samuels, I. S., Martemyanov, K. A., . . . Gregg,  
610 R. G. (2014). GPR179 is required for high sensitivity of the mGluR6 signaling cascade in  
611 depolarizing bipolar cells. *J Neurosci*, *34*(18), 6334-6343. doi:10.1523/JNEUROSCI.4044-  
612 13.2014
- 613 Rosenbaum, D. M., Rasmussen, S. G., & Kobilka, B. K. (2009). The structure and function of G-  
614 protein-coupled receptors. *Nature*, *459*(7245), 356-363. doi:10.1038/nature08144
- 615 Smith, E. L., Harrington, K., Staehr, M., Masakayan, R., Jones, J., Long, T. J., . . . Brentjens, R.  
616 J. (2019). GPRC5D is a target for the immunotherapy of multiple myeloma with rationally  
617 designed CAR T cells. *Sci Transl Med*, *11*(485). doi:10.1126/scitranslmed.aau7746
- 618 Sriram, K., & Insel, P. A. (2018). G Protein-Coupled Receptors as Targets for Approved Drugs:  
619 How Many Targets and How Many Drugs? *Mol Pharmacol*, *93*(4), 251-258.  
620 doi:10.1124/mol.117.111062
- 621 Stoppel, L. J., Auerbach, B. D., Senter, R. K., Preza, A. R., Lefkowitz, R. J., & Bear, M. F. (2017).  
622 beta-Arrestin2 Couples Metabotropic Glutamate Receptor 5 to Neuronal Protein Synthesis  
623 and Is a Potential Target to Treat Fragile X. *Cell Rep*, *18*(12), 2807-2814.  
624 doi:10.1016/j.celrep.2017.02.075
- 625 Sutton, L. P., Orlandi, C., Song, C., Oh, W. C., Muntean, B. S., Xie, K., . . . Martemyanov, K. A.  
626 (2018). Orphan receptor GPR158 controls stress-induced depression. *Elife*, *7*.  
627 doi:10.7554/eLife.33273
- 628 Wang, D., Stoveken, H. M., Zucca, S., Dao, M., Orlandi, C., Song, C., . . . Martemyanov, K. A.  
629 (2019). Genetic behavioral screen identifies an orphan anti-opioid system. *Science*,  
630 *365*(6459), 1267-1273. doi:10.1126/science.aau2078
- 631 Watkins, L. R., & Orlandi, C. (2020). Orphan G Protein Coupled Receptors in Affective Disorders.  
632 *Genes (Basel)*, *11*(6). doi:10.3390/genes11060694

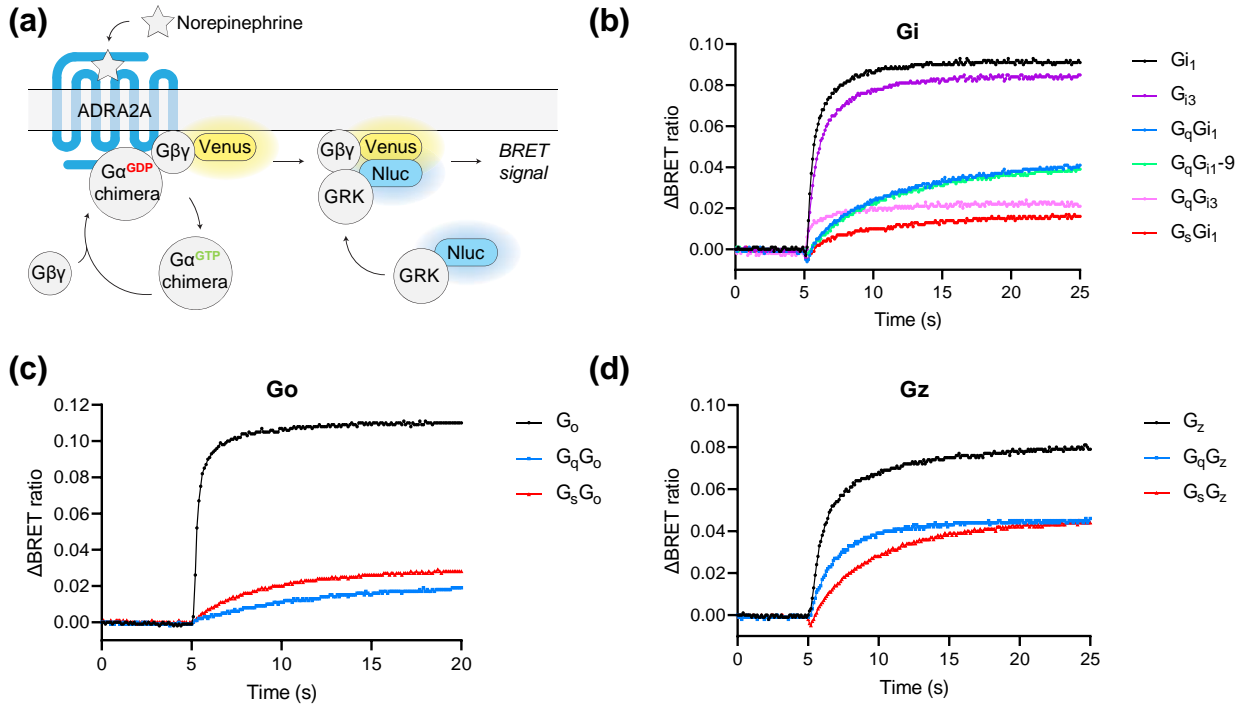
633

**Fig.1**

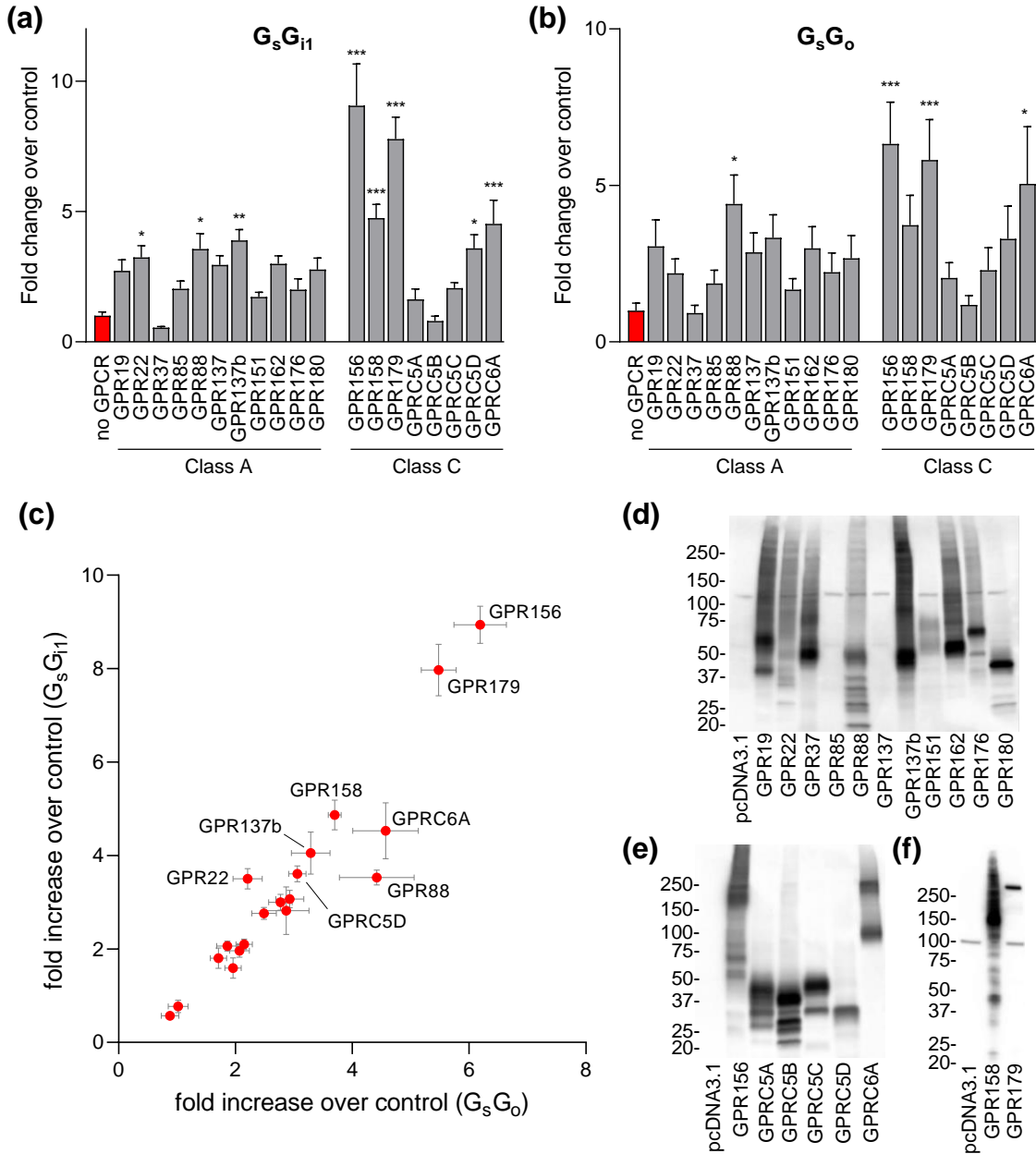
**Figure 1. Analysis of GPCR constitutive activity.** 4 luciferase reporter assays were used to measure the constitutive activity of a library of 41 GPCRs that include 19 orphan GPCRs. The amount of firefly luciferase accumulated in the cells was normalized on the levels of constitutively expressed renilla luciferase. The effect of GPCR overexpression was compared to cells expressing only the reporters (control cells, dotted line) and reported as fold-change over control. Colors are used to discriminate know G protein coupling:  $G_s$  (yellow),  $G_q$  (orange),  $G_{12/13}$  (blue), and  $G_{i/o}$  (green). oGPCRs are in gray. (a) NFAT-RE-induced luciferase expression. (b) CRE-induced luciferase expression. (c) SRE-induced luciferase expression. (d) SRF-RE-induced luciferase expression. The data shown represent the average of 3-6 independent experiments, each performed in duplicate. Data shown as means  $\pm$  SEM.

**Fig.2**

**Figure 2. Use of G protein chimeras to detect constitutive  $G_{i/o}$  activation.** (a) Sequence alignment of the last 14 amino acids of wild type G proteins (top),  $G_q$ -derived chimeras (middle), and  $G_s$ -derived chimeras (bottom). Residues conserved among every G protein are highlighted in gray. Residues that were substituted in the G protein chimeras were highlighted and aligned with the G protein C-terminal sequence of the core protein ( $G_q$ , middle;  $G_s$ , bottom). (b) Constitutive activation of  $G_q$  chimeras by overexpression of GRM2. Reported is the fold change over control cells expressing only NFAT-Nluc reporter and renilla luciferase (dotted line). (c) Constitutive activation of  $G_s$  chimeras activate by GRM2 and reported as fold change over control cells expressing only CRE-Nluc reporter and renilla luciferase (dotted line). (d) Analysis of the constitutive activity of the  $G_{i/o}$ -coupled metabotropic glutamate receptors GRM2, GRM3, GRM4, GRM6, GRM7, and GRM8, the  $\alpha 2A$ -adrenergic receptor (ADRA2A), and the serotonin 1A receptor (HTR1A) with each of the 8  $G_q$ - and  $G_s$ -based chimeras. The data shown represent the average of 3 (panels b and c) or 3-6 (panel d) independent experiments, each performed in duplicate. Data shown as means  $\pm$  SEM.

**Fig.3**

**Figure 3. G protein chimera activation by agonist-activated GPCRs using BRET assay.** (a) Schematic representation of the BRET assay used to detect agonist-induced activation of ADRA2A. Norepinephrine application triggers the GDP exchange with GTP on the  $G\alpha$  subunit and the subsequent dissociation of  $G\beta\gamma$ -Venus. At the membrane, released  $G\beta\gamma$  will interact with the C-terminus of masGRK3 that is fused with Nanoluc. Using a BMG Omega plate reader we can therefore detect the BRET signal generated. (b) Representative response profile showing the BRET signal after norepinephrine application at 5 seconds. The  $\Delta$ BRET ratio is calculated for each of the wild type  $G_{i1}$  and  $G_{i3}$ , or the chimeric G proteins bearing a  $G_{i1}$  or  $G_{i3}$  C-terminus. (c) Norepinephrine activation of wild type  $G_o$  or G protein chimeras with a  $G_o$  C-terminus. (d) Norepinephrine activation of wild type  $G_z$  or G protein chimeras with a  $G_z$  C-terminus. The data shown were replicated in 3 independent experiments.

**Fig.4**

**Figure 4. Orphan GPCR screening for  $G_{i/o}$  coupling.** Quantification of luciferase expression in cells co-transfected with oGPCRs,  $G_s$ -based chimeras, CRE-Nluc, and renilla luciferase showed as fold change over control cells not overexpressing oGPCRs. (a) Analysis of constitutive activation of the  $G_sG_{i1}$  chimera by class A and class C oGPCRs. (b) Constitutive activation of the  $G_sG_o$  chimera by class A and class C oGPCRs. (c) Bi-dimensional representation of oGPCR  $G_{i/o}$  constitutive activity. Only oGPCRs showing statistically significant activity are labeled. The data shown represent the average of 4 ( $G_sG_{i1}$ ) or 5 ( $G_sG_o$ ) independent experiments, each performed in duplicate (one-way ANOVA with Dunnett's multiple comparisons test, \* $p < 0.05$ , \*\* $p < 0.01$ , \*\*\* $p < 0.001$ ). Data are shown as means  $\pm$  SEM. (d-f) Western blot analysis of protein levels detected in cells transfected with oGPCRS or without (pcDNA3.1) as a negative control. Antibodies raised against HA tag were used to detect class A oGPCRs (d), and some class C oGPCRs (e). Antibodies against myc tag were used to detect class C GPR158 and GPR179 (f).

**Fig.5**

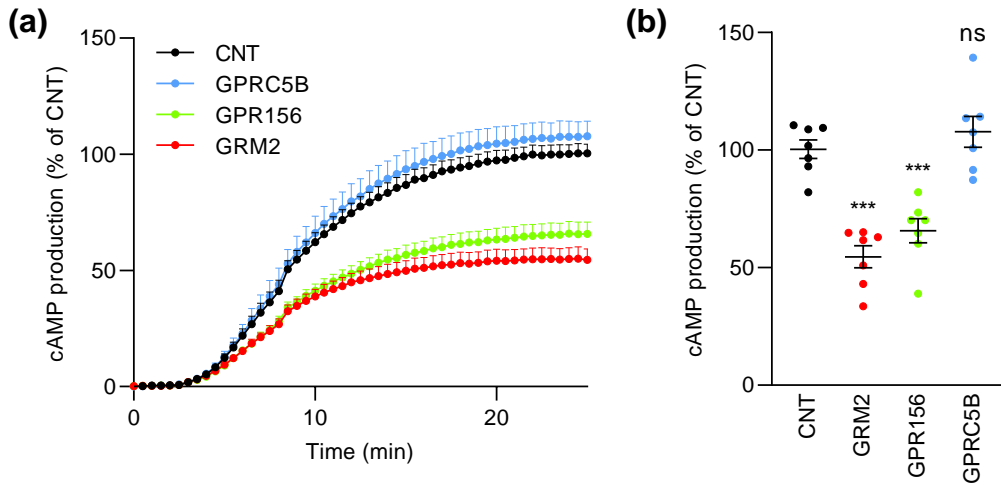


**Figure 5.  $G_{i/o}$  coupling validation for GPR156.** (a) cAMP production induced by 0.5  $\mu$ M forskolin treatment at 3 minutes. (b) Quantification of the forskolin-induced amplitude reported in panel (a). Cells overexpressing GPR156 and GRM2 show a constitutive inhibition of cAMP production while cells transfected with GPRC5B are not significantly different from control cells transfected with empty vector. Data are shown as means  $\pm$  SEM ( $n = 7$  independent experiments; one-way ANOVA with Dunnett's multiple comparisons test, \*\*\* $p < 0.001$ ).